Journal of Power Sources 196 (2011) 6502–6506

Contents lists available at ScienceDirect

Journal of Power Sources

journal homepage: www.elsevier.com/locate/jpowsour

Short communication

Li/$LiFePO_4$ batteries with gel polymer electrolytes incorporating a guanidinium-based ionic liquid cycled at room temperature and 50 °C

Mingtao Li[a], Li Yang[a,b,*], Shaohua Fang[a], Siming Dong[a], Yide Jin[a], Shin-ichi Hirano[b], Kazuhiro Tachibana[c]

[a] School of Chemistry and Chemical Technology, Shanghai Jiaotong University, Shanghai 200240, China
[b] Hirano Institute for Materials Innovation, Shanghai Jiaotong University, Shanghai 200240, China
[c] Department of Chemistry and Chemical Engineering, Faculty of Engineering, Yamagata University, Yamagata 992-8510, Japan

ARTICLE INFO

Article history:
Received 19 November 2010
Received in revised form 28 February 2011
Accepted 28 March 2011
Available online 6 April 2011

Keywords:
Lithium metal polymer battery
Gel polymer electrolytes
Guanidinium-based ionic liquid

ABSTRACT

Gel polymer electrolytes composed of PVdF-HFP microporous membrane incorporating a guanidinium-based ionic liquid with 0.8 mol kg^{-1} lithium bis(trifluoromethanesulfonylimide) are characterized as the electrolytes in Li/$LiFePO_4$ batteries. The ionic conductivity of these gel polymer electrolytes is 3.16×10^{-4} and 8.32×10^{-4} S cm^{-1} at 25 and 50 °C, respectively. The electrolytes show good interfacial stability towards lithium metal and high oxidation stability, and the decomposition potential reaches 5.3 and 4.6 V (vs. Li/Li^+) at 25 and 50 °C, respectively. Li/$LiFePO_4$ cells using the PVdF-HFP/1g13TFSI-LiTFSI electrolytes show good discharge capacity and cycle stability, and no significant loss in discharge capacity of the battery is observed over 100 cycles. The cells deliver the capacity of 142 and 150 mAh g^{-1} at the 100th cycling at 25 and 50 °C, respectively.

1. Introduction

Lithium metal polymer batteries (LMPBs) have been considered as the most probably next generation of power sources for portable electronic devices and hybrid electric vehicles because of their high-energy density and flexible characteristics [1,2]. However, the performance of LMPBs is still limited by the poor ionic conductivity of the solid polymer electrolytes at room temperature. To elevate the ionic conductivity, gel polymer electrolytes are prepared by incorporating organic carbonate solvents in the host polymer, i.e., ethylene carbonate (EC), propylene carbonate (PC), diethyl carbonate (DEC) or ϒ-butyrolactone [3,4]. However, the highly reactive lithium metal cannot be thermodynamically compatible with the organic carbonate solvents. In addition, these flammable organic solvents employed in lithium batteries are recognized as one of the main causes of the serious safety drawbacks [5].

Recently, a very promising approach appears to be the incorporation of ionic liquids (ILs) into polymer electrolytes [6–8]. ILs are room temperature molten salts typically consisting of bulky, asymmetric organic cations and inorganic anions. The interest in these materials arises from their desirable properties such as non-volatility, non-flammability, high ionic conductivity, high thermal stability, and a wide electrochemical window. Hence, variety of ILs have been synthesized and incorporated into polymer electrolytes. Among them, families of imidazolium-based and pyrrolidinium-based ILs have been widely studied because of their low viscosity, high room temperature conductivity, high solubility of lithium salts and high anodic stability [6,9–11]. However, these imidazolium-based ILs have low cathodic stability and an unfavorable compatibility towards the lithium metal anode due to the presence of acidic protons and double bonds in the cation. So, small quantities of film-forming additives have to be added in the electrolyte to avoid its cathodic decomposition and improve the interfacial compatibility towards the lithium anode [12,13]. In comparison with the imidazolium-based ILs, pyrrolidinium-based ILs show a much wider cathodic decomposition potential and better compatibility towards the lithium anode. Electrochemical properties of the incorporation of several *N*-alky-*N*-methypyrrolidinium bis(trifluoromethane-sulfonyl)imide (PYR_{1A}TFSI) ILs into PEO-based electrolytes system had been reported [9]. The addition of PYR_{1A}TFSI enhanced the ionic conductivity of PEO-based electrolytes over 10^{-4} S cm^{-1}. Battery tests had shown that Li/$P(EO)_{10}$LiTFSI + 0.96 PYR_{1A}TFSI/$LiFePO_4$ cells were capable of delivering a capacity of 125 and 100 mAh g^{-1} at 30 and 25 °C, respectively. The addition of the PYR_{14}TFSI to the $P(EO)_{10}$LiTFSI polymer electrolytes resulted in a significant enhancement of the ionic conductivity [14]. Li/$LiFePO_4$ cells making use of this new family of polymer electrolytes at 20 °C could deliver 138 mAh g^{-1} during the first discharge. PVdF-HFP composite membranes incorporated LiTFSI, ether-functionalized

* Corresponding author. Tel.: +86 21 54748917; fax: +86 21 54741297.
E-mail address: liyang@sjtu.edu.cn (L. Yang).

0378-7753/$ – see front matter © 2011 Elsevier B.V. All rights reserved.
doi:10.1016/j.jpowsour.2011.03.071

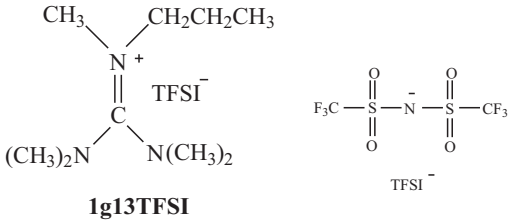

1g13TFSI

Scheme 1. Structure of the guanidinium-based IL used in the gel polymer electrolyte.

pyrrolidinium-imide IL ($PYRA_{12o1}TFSI$) and different silica had been prepared [15]. The Li/$LiFePO_4$ cells with PVdF-HFP/ $PYRA_{12o1}TFSI$-LiTFSI film containing 10 wt% of mesoporous SiO_2 showed good charge/discharge capacity and low capacity losses at medium C-rates.

Our group has recently synthesized a series of guanidinium-based ILs with low viscosity and some of them were used as new electrolytes for Li/$LiCoO_2$ cell without additives [16–18]. The cells showed high coulombic efficiency, good discharge capacity and stable cycle property at 0.2 C current rates. Compared with liquid electrolytes, gel polymer electrolytes reduce the possibility of the liquid leakage and furthermore, the use of gel polymer electrolytes enables fabrication of thin batteries with flexible design. [15] In this article we prepared a new polymer electrolyte, the PVdF-HFP microporous membrane incorporating a guanidinium-based IL denoted 1g13TFSI (see Scheme 1). 1g13TFSI was used as the electrolyte in this work because in comparison with the other guanidinium-based ILs electrolyte, cells by it have a higher delivered capacity and better cycle stability. The performance of these polymer electrolytes in Li/$LiFePO_4$ batteries cycling at room temperature and 50 °C is reported.

2. Experimental

2.1. Synthesis of 1g13TFSI and preparation of 1g13TFSI–LiTFSI solution

The structure of guanidinium-based IL used in this study was shown in Scheme 1 and the IL was prepared according to our reported method [16,17]. The IL was dried under high vacuum for more than 24 h at 105 °C before using. The water content of the dried IL was detected by a moisture titrator (Metrohm73 KF coulometer) basing on Karl-Fischer method, and the value was less than 50 ppm. Then 0.8 mol kg^{-1} of LiTFSI-1g13TFSI (LiTFSI kindly provided by Morita Chemical Industries Co., Ltd.) was obtained by adding the LiTFSI to the dried IL. And this procedure was carried out in an argon-filled glove box ([O_2] < 1 ppm, [19] < 1 ppm).

2.2. Preparation of the gel polymer electrolyte membranes

A porous poly(vinylidene fluoride-*co*-hexafluoropropylene), PVdF-HFP, membrane was prepared as follows. PVdF-HFP (Kynar, 2801), *N*,*N*-dimethylacetamide and Polyvinyl pyrolidone (PVP, K-30) in the weight ratio of 1:10:0.4 were mixed together at 60 °C for 8 h and then cast to the thickness of 200 μm using a doctor blade. PVP was used as a plasticizer for the formation of pores in the membrane when it was immersed in water. After 30 min, the membranes were immersed in deionized water to remove PVP. Then the membranes were vacuum dried at 80 °C for 20 h. The gel polymer electrolytes were prepared by the immersion of the porous PVdF-HFP membranes in a 0.8 mol kg^{-1} 1g13TFSI–LiTFSI solution for 2 h.

2.3. Characterization of the gel polymer electrolyte membranes

Sample morphology was investigated using a Hitachi S4700 field emission scanning electron microscope (FESEM). Electrochemical stability was determined by the linear sweep voltammetry (LSV) of a Li/the electrolyte membrane/SS cell at a scan rate of 10 mVs^{-1} over the range of open-circuit voltage to 7.0 V. The decomposition voltage onset was set as the current density was up to 0.1 mA cm^{-2} [20].

The ionic conductivity of the samples was measured by sandwiching the samples between two stainless steel blocking electrodes using AC impedance techniques. The measurements were performed using an CHI660B Electrochemical Workstation between 100 kHz and 10 Hz at various temperatures ranging from 25 to 80 °C. A thermostatic equipment (Jinghua Co., Ltd. Shanghai, China) was utilized to control the temperature within ±0.1 °C of the target value. The samples were thermally equilibrated at each temperature for at least 1 h prior to the measurements. The bulk resistance (R_b) was obtained by reading the intercept of the impedance spectrum, and the ion conductivity was calculated from the expression $\sigma = L/(R_bA)$ where L is the thickness of the electrolyte film and A represents the electrode area.

The interfacial resistance (R_f) between the gel polymer electrolyte membrane and lithium metal electrode was measured by the impedance response of Li/polymer electrolyte/Li cells. The R_f measurements were carried out over the frequency range from 10 to 1 MHz at an amplitude of 20 mV with the polymer electrolyte separator having an area of 2 cm^2 and Li metal having an area of 1.8 cm^2. Cyclic voltammetry (CV) of the gel polymer electrolyte membrane sandwiched between lithium electrodes was measured at 25 and 50 °C at a scan rate of 10 mV s^{-1} between −1 and +1 V, respectively.

2.4. Evaluation of the performance of cells

Li/$LiFePO_4$ coin cell was used to evaluate the performance of the gel polymer electrolytes in lithium battery applications. Lithium foil (battery grade) was used as a negative electrode. The thickness and surface area of the lithium foil were 1.2 mm and 1.54 cm^2, respectively. The positive electrode was fabricated by spreading the mixture of $LiFePO_4$, acetylene black and PVdF (initially dissolved in *N*-methyl-2-pyrrolidone) with a weight ratio of 8:1:1 onto Al current collector (battery use). Loading of active material was about, ca. 2.0–2.5 mg cm^{-2} and this thinner electrode was directly used without pressing. Cell construction was carried out in the glove box, and all the components of cell were dried under vacuum before placed into the glove box. Cell performance was examined by the galvanostatic charge–discharge (C–D) cycling test using a CT2001A cell test instrument (LAND Electronic Co., Ltd.) at 25 and 50 °C. The cells were sealed and then stayed at determining temperature for 12 h before the performance test. Current rate was determined by using the nominal capacity of 150 mAh g^{-1} for Li/ $LiFePO_4$ cell. Charge included two processes: (1) constant current at a rate, cut-off voltage of 4.0 V and (2) constant voltage at 4.0 V, setting time of 2 h, and discharge had one process: constant current at different rates, cut-off voltage of 2.5 V.

3. Results and discussion

3.1. Morphology of the membranes

Fig. 1 shows SEM microscopic images of a pure PVdF-HFP and a PVdF-HFP/1g13TFSI-LiTFSI gel polymer electrolyte membrane. The pure PVdF-HFP membrane was opaque in appearance and did not show discernable pore structure in the SEM image as shown

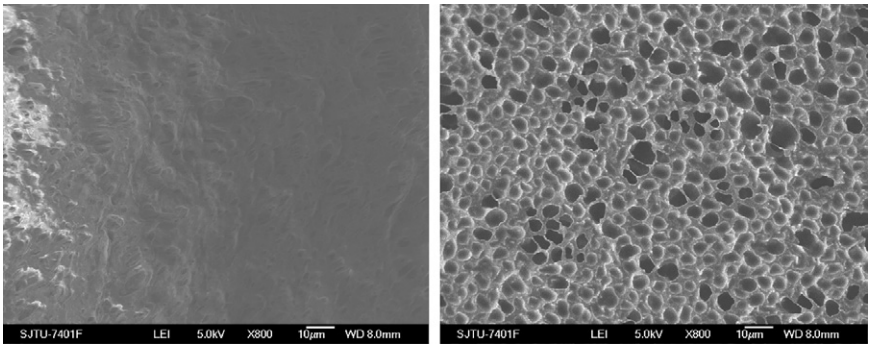

Fig. 1. SEM images of (a) a pure PVdF-HFP membrane and (b) a PVdF-HFP/1g13TFSI-LiTFSI gel polymer electrolyte membrane.

in Fig. 1(a). After the PVdF-HFP membrane was immersed in the 1g13TFSI–LiTFSI solution, the membrane changed transparent in appearance and large quantities of homogeneous pores were found in the SEM image as shown in Fig. 1(b). The high porosity of the membranes was also reflected in their high electrolyte solution with 670 wt% obtained for the PVdF-HFP membranes. It was found, like in the other literature [21], that electrolyte uptake was higher for the membrane having higher porosity. In other words, the electrolyte uptake and ionic conductivity increased with porosity. The observed pore size was calculated to be 2–8 μm. The pore size and homogeneity were related to the content of the PVP which was used as a plasticizer for the formation of pores in the membrane when it was immersed in deionized water. The PVP content of 4 wt.% around was suitable as previously described [22,23]. The large and uniformly dispersed pores in the membrane microstructure lead to the high retention of ILs and thereby connectivity through the membrane that gives rise to high ionic conductivity.

3.2. Ionic conductivity and electrochemical stability

Fig. 2 shows the temperature dependence of ionic conductivity of the PVdF-HFP/1g13TFSI-LiTFSI gel polymer electrolyte membrane at different temperatures by the AC impedance method. For the sample, a linear increase was observed in the conductivity values with temperature, which characterized the ionic conductivity mechanism as an Arrhenius-type behavior. In gel polymer electrolyte system, the change of conductivity with temperature may be due to the segmental motion of the polymer chains leading to increase in free volume in the system, which will provide an easy pathway for the transitional motion of the ions. The segmental motion also permits the ions to hop from one site to another. As the temperature increases, both the segmental motion and transitional ionic motion in the system will increase due the high activation energy, and it will improve the ionic conductivity [24]. The PVdF-HFP/1g13TFSI-LiTFSI gel polymer electrolyte reported here exhibited higher ionic conductivity above 3.16×10^{-4} and 8.32×10^{-4} S cm^{-1} at 25 and 50 °C respectively, which made them suitable for the application in lithium polymer batteries at moderate temperature.

The PVdF-HFP/1g13TFSI-LiTFSI membranes had good oxidation stability at 25 and 50 °C from their electrochemical stability window as shown in Fig. 3. It can be seen from Fig. 3 that the decomposition potential limit (here the potential was set at a current density up to 0.1 mA cm^{-2}) of the PVdF-HFP/1g13TFSI-LiTFSI membrane reached 5.3 V (vs. Li/Li$^+$) at 25 °C. As the temperature increased, the oxidation stability of the PVdF-HFP/1g13TFSI-LiTFSI membrane decreased and the membrane decomposed at about 4.6 V (vs. Li/Li$^+$) at 50 °C. The large and fully interconnected pores, high porosity, higher specific surface and uniform morphology of the membranes were also contributed to the electrochemical stability of the gel polymer electrolytes. The earlier studies were reported on high electrochemical stability of PVdF-HFP based gel polymer electrolytes as well [25]. The oxidation stability of the gel polymer electrolyte membrane reflects its stability on cathode of a lithium polymer battery, which is important for the application of high voltage cathode materials.

3.3. Interfacial stability

Fig. 4 shows the time evolution of the impedance spectra of a symmetrical Li/(PVdF-HFP/1g13TFSI-LiTFSI)/Li cell over storage up to 7 days at 25 and 50 °C under open-circuit conditions. The intercept with real axis of the spectra at high frequency was assigned to the electrolyte bulk resistance, and the diameter of the semicircle was assigned to the interfacial resistance (R_i) of the gel polymer electrolyte/lithium metal. For the PVdF-HFP/1g13TFSI-LiTFSI gel

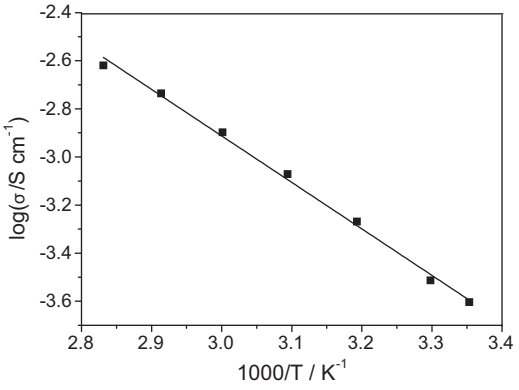

Fig. 2. Temperature dependence of the ionic conductivity of the PVdF-HFP/1g13TFSI-LiTFSI gel polymer electrolyte membrane.

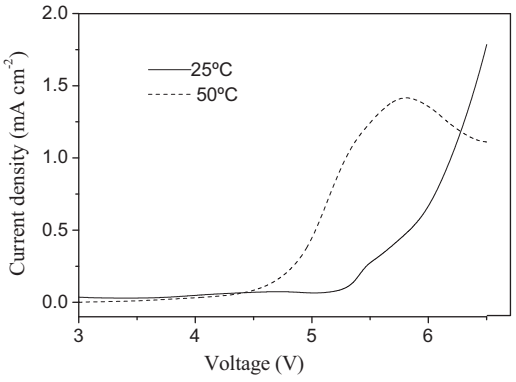

Fig. 3. Oxidation stability by linear sweep voltammetry of the PVdF-HFP/1g13TFSI-LiTFSI electrolyte membrane at 25 and 50 °C (Li/polymer electrolyte/SS cell, 10 mV s^{-1}, 3–7 V).

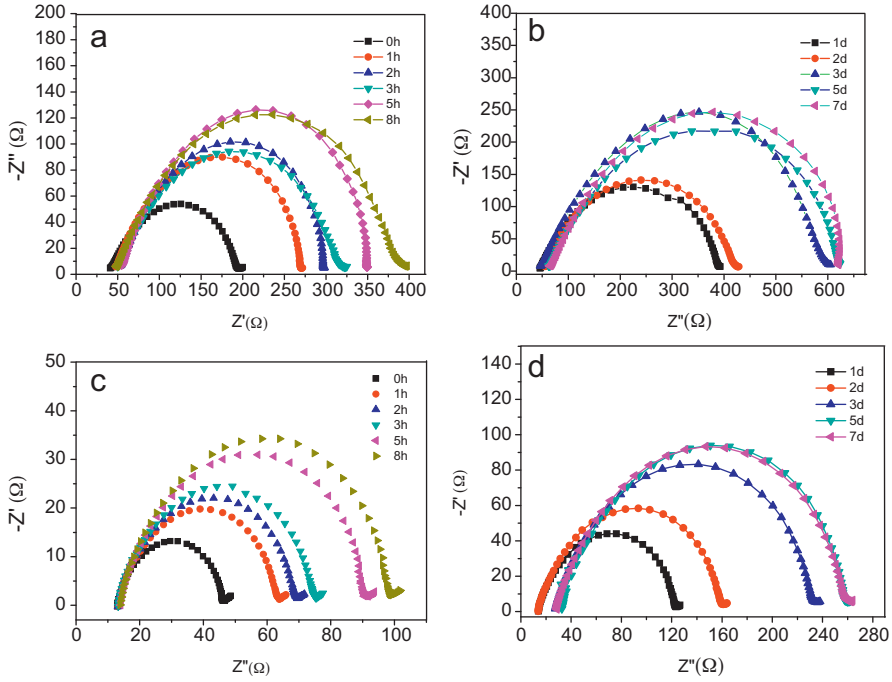

Fig. 4. Time evolution of the impedance spectra of symmetrical Li/(PVdF-HFP/1g13TFSI-LiTFSI)/Li cells: (a) from 0 to 10 h at 25 °C, (b) from 1 to 7 days at 25 °C, (c) from 0 to 10 h at 50 °C and (d) from 1 to 7 days at 50 °C.

electrolyte, its bulk resistance was almost unchanged with time during 7 days. Fig. 4(a) and (c) show the R_i values grew continuously from 0 to 8 h at 25 and 50 °C, indicating the occurrence of a reaction between the lithium metal and the polymer electrolyte with the formation of a passivating layer. In Fig. 4(b) and (d), the R_i values also grew continuously over the storage time and it remain more or less constant after 5 days on the value of 620 and 260 Ω at 25 and 50 °C, respectively. The cathodic limiting potential of 1g13TFSI was about 0.7 V vs. Li/Li^+ [16], so it was very possible that this IL could continuously react with lithium metal. However, the evolution of the impedance spectra might indicate that the polymer electrolyte reacted with lithium metal and a solid electrolyte interface (SEI) layer was formed at the same time, as seen in other literatures [6,24,26]. The SEI layer restricted the reaction between the polymer electrolyte and lithium metal gradually, and a dynamic equilibrium could be achieved after some time.

Curves of cyclic voltammograms of the symmetrical Li/(PVdF-HFP/1g13TFSI-LiTFSI)/Li cells exhibited clear anodic and cathodic peaks as shown in Fig. 5. In the first cycle for the PVdF-HFP/1g13TFSI-LiTFSI polymer electrolyte at 25 °C, the plating of lithium was at about −0.60 V vs. Li/Li^+, and the anodic peak at about 0.63 V vs. Li/Li^+ in the returning scan corresponded to the stripping of lithium. The lithium redox in this electrolyte could be caused by the generation of a SEI film on the surface of the

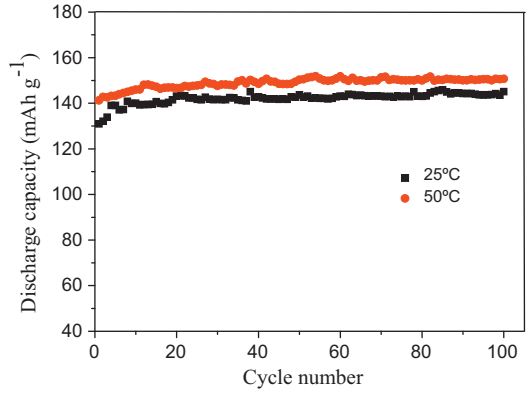

Fig. 6. Discharge capacity as a function of cycle number for Li/(PVdF-HFP/1g13TFSI-LiTFSI)/$LiFePO_4$ cells at 25 and 50 °C. Charge–discharge current rate is 0.1 C.

lithium. The peak currents of the lithium redox decreased gradually with the cycle number, and it suggested that the SEI film had being formed so that the lithium redox was restrained markedly. After the 10th circle, the peak currents retained constant which suggested a stable SEI film was formed. Following the initial stabilization, the cell showed overlapping CV curves on cycling and the anodic and cathodic peak current values were also nearly the same,

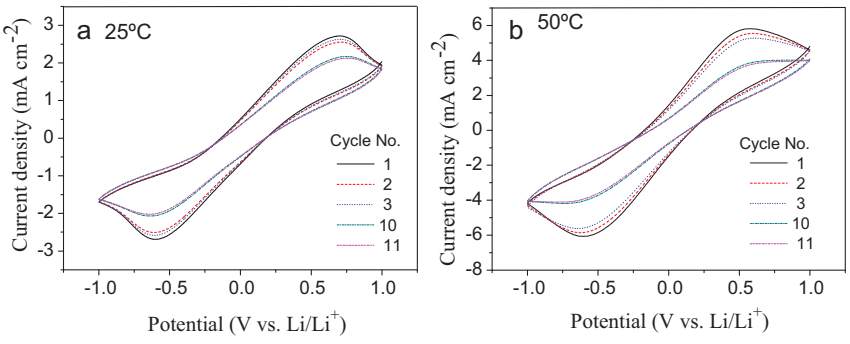

Fig. 5. Cyclic voltammograms of symmetrical Li/(PVdF-HFP/1g13TFSI-LiTFSI)/Li cells, scan rate: 10 mV s^{-1}.

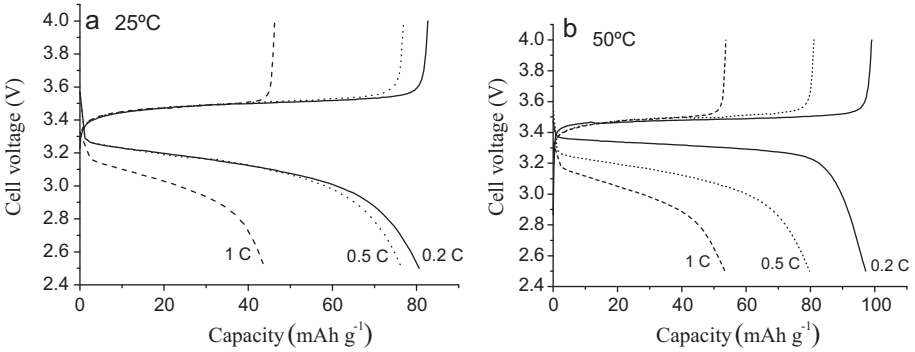

Fig. 7. Voltage vs. discharge profile of Li/(PVdF-HFP/1g13TFSI-LiTFSI)/$LiFePO_4$ cells at 25 and 50 °C. Charge current rate is fixed at 0.1 C and discharge current rate is indicated in the figure.

which indicated the occurrence of reversible redox processes and high coulombic efficiency of the redox process.

3.4. Battery performance

The performance of Li/(PVdF-HFP/1g13TFSI-LiTFSI)/$LiFePO_4$ cells had been characterized at room temperature and 50 °C and the rates of charge and discharge were 0.1 C (corresponding to 0.04 mA cm^{-2}), and their cycling properties were presented in Fig. 6. The discharge capacity was found to be 131 and 142 mAh g^{-1} in the first cycle at 25 and 50 °C, respectively. The capacity of the cell increased gradually during the first 10–15 cycles, perhaps as a result of generation of improved penetration and contact of the IL component from the electrolyte into the electrode material [27]. After that, the discharge capacity kept steady essentially and the values were about 142 and 150 mAh g^{-1} at 25 and 50 °C, respectively, and no significant loss of the discharge capacity was observed over 100 cycles. The reason that the cell delivers higher capacity at 50 °C probably is that the ionic conductivity and interface compatibility are better at elevated temperature.

The discharge capacities at different current rates for Li/(PVdF-HFP/1g13TFSI-LiTFSI)/$LiFePO_4$ cells at 25 and 50 °C were also measured. As shown in Fig. 7, it could be found that the discharge capacity decreased drastically with increasing the current rates. As is known, the IL electrolytes are made up by Li^+ and other varieties of ions such as ion complexes and the transport of those ion complexes may lead to cell polarization, which will reduce the rate performance of the lithium batteries [20]. However, it had been proved that the high lithium salt concentration in the electrolyte was beneficial for the rate capability of the lithium batteries owing to the improvement of the lithium ion transport number. But the lithium salt concentration could not be too high because it led to low ionic conductivity due to high ionic association.

4. Conclusion

Ionic liquids thermodynamically compatible with lithium metal are very promising for applications to rechargeable lithium metal polymer batteries. In this article, gel polymer electrolytes composed of PVdF-HFP microporous membrane incorporating a guanidinium-based ionic liquid with 0.8 mol kg^{-1} lithium bis(trifluoromethanesulfonylimide) are prepared as the electrolytes in Li/$LiFePO_4$ cells. The PVdF-HFP/1g13TFSI-LiTFSI gel polymer electrolytes exhibit higher ionic conductivity above 3.16×10^{-4} and 8.32×10^{-4} S cm^{-1} at 25 and 50 °C respectively. The gel polymer electrolytes have good chemical stability towards lithium metal and high oxidation stability, and the anodic limiting potential of the electrolyte is 5.3 and 4.6 V (vs. Li/Li^+) at 25 °C and 50 °C. Li/$LiFePO_4$ cell using the PVdF-HFP/1g13TFSI-LiTFSI electrolytes shows good discharge capacity and cycle stability, and no significant loss in discharge capacity of the battery is observed over 100 cycles. The cell delivers the capacity of 142 and 150 mAh g^{-1} at the 100th cycling at 25 and 50 °C, respectively.

Acknowledgements

The authors thank the research center of analysis and measurement of Shanghai Jiao Tong University for the help in the NMR characterization. This work was financially supported by the National Key Project of China for Basic Research under grant no. 2006CB202600, the National High Technology Research and Development Program of China under grant no. 2007AA03Z222.

References

[1] J.M. Tarascon, M. Armand, Nature 414 (2001) 359.
[2] M. Armand, J.M. Tarascon, Nature 451 (2008) 652.
[3] K.M. Abraham, Z. Jiang, J Electrochem. Soc. 143 (1996) 1.
[4] J. Read, J Electrochem. Soc. 149 (2002) A1190.
[5] K.-S. Liao, T.E. Sutto, E. Andreoli, P. Ajayan, K.A. McGrady, S.A. Curran, J. Power Sources 195 (2010) 867.
[6] P. Raghavan, X. Zhao, J. Manuel, G.S. Chauhan, J.-H. Ahn, H.-S. Ryu, H.-J. Ahn, K.-W. Kim, C. Nah, Electrochim. Acta 55 (2010) 1347.
[7] D.W. Kim, S.R. Sivakkumar, D.R. MacFarlane, M. Forsyth, Y.K. Sun, J. Power Sources 180 (2008) 591.
[8] M. Galiński, A. Lewandowski, I. Stepniak, Electrochim. Acta 51 (2006) 5567.
[9] G.T. Kim, G.B. Appetecchi, F. Alessandrini, S. Passerini, J. Power Sources 171 (2007) 861.
[10] J.H. Shin, W.A. Henderson, S. Scaccia, P.P. Prosini, S. Passerini, J. Power Sources 156 (2006) 560.
[11] Y.S. Fung, R.Q. Zhou, J. Power Sources 81–82 (1999) 891.
[12] V.R. Koch, C. Nanjundiah, G. Battista Appetecchi, B. Scrosati, J. Electrochem. Soc. 142 (1995).
[13] H. Matsumoto, M. Yanagida, K. Tanimoto, M. Nomura, Y. Kitagawa, Y. Miyazaki, Chem. Lett. (2000) 922.
[14] J.H. Shin, W.A. Henderson, C. Tizzani, S. Passerini, S.S. Jeong, K.W. Kim, J. Electrochem. Soc. 153 (2006).
[15] S. Ferrari, E. Quartarone, P. Mustarelli, A. Magistris, M. Fagnoni, S. Protti, C. Gerbaldi, A. Spinella, J. Power Sources 195 (2010) 559.
[16] S.H. Fang, L. Yang, J.X. Wang, H.Q. Zhang, K. Tachibana, K. Kamijima, J. Power Sources 191 (2009) 619.
[17] S.H. Fang, L. Yang, C. Wei, C. Jiang, K. Tachibana, K. Kamijima, Electrochim. Acta 54 (2009) 1752.
[18] S.H. Fang, L. Yang, J.X. Wang, M.T. Li, K. Tachibana, K. Kamijima, Electrochim. Acta 54 (2009) 4269.
[19] Y.H. Chen, Y.G. Wang, Q.Y. Cheng, X.L. Liu, S.J. Zhang, J. Chem. Thermodyn. 41 (2009) 1056.
[20] H. Ye, J. Huang, J.J. Xu, A. Khalfan, S.G. Greenbaum, J. Electrochem. Soc. 154 (2007).
[21] H.S. Jeong, D.W. Kim, Y.U. Jeong, S.Y. Lee, J. Power Sources 195 (2010) 6116.
[22] J.H. Cao, B.K. Zhu, Y.Y. Xu, Chin. J. Polym. Sci. (English Edition). 24 (2006) 205.
[23] L. Shi, R. Wang, Y. Cao, C. Feng, D.T. Liang, J.H. Tay, J. Membr. Sci. 305 (2007) 215.
[24] P. Raghavan, X. Zhao, C. Shin, D.H. Baek, J.W. Choi, J. Manuel, M.Y. Heo, J.H. Ahn, C. Nah, J. Power Sources 195 (2010) 6088.
[25] K. Han, D. Lu, Fuhe Cailiao Xuebao/Acta Materiae Compositae Sinica 25 (2008) 57.
[26] A. Fernicola, F. Croce, B. Scrosati, T. Watanabe, H. Ohno, J. Power Sources 174 (2007) 342.
[27] S.Y. Chew, J. Sun, J. Wang, H. Liu, M. Forsyth, D.R. MacFarlane, Electrochim. Acta 53 (2008) 6460.